

Enhanced HCN(1–0) Emission in the Type-1 Seyfert Galaxy NGC 1097

Kotaro KOHNO,¹ Sumio ISHIZUKI,² Satoshi MATSUSHITA,³
Baltasar VILA-VILARÓ,⁴ and Ryohei KAWABE²

¹*Institute of Astronomy, The University of Tokyo, Osawa, Mitaka, Tokyo, 181-8588*

kkohno@ioa.s.u-tokyo.ac.jp

²*National Astronomical Observatory, Osawa, Mitaka, Tokyo, 181-8588*

³*Submillimeter Array, Harvard-Smithsonian Center for Astrophysics,
P.O. Box 824, Hilo, HI 96721- 0824, U.S.A.*

⁴*Steward Observatory, The University of Arizona, Tucson, AZ 85721, U.S.A.*

(Received ; accepted)

Abstract

The central kpc region of the low luminosity type-1 Seyfert galaxy NGC 1097 has been observed in the CO(1–0) and HCN(1–0) lines with the Nobeyama Millimeter Array and the NRO 45 m telescope. We find a striking enhancement of the HCN emission toward the active nucleus of NGC 1097; a large fraction of the CO emission comes from the circumnuclear starburst ring ($r \sim 10''$ or 700 pc at $D = 14.5$ Mpc), whereas the HCN emission is dominated by a strong unresolved peak at the nucleus. The HCN-to-CO integrated intensity ratio in brightness temperature scale, $R_{\text{HCN/CO}}$, is about 0.11 in the aperture of the 45 m telescope beams ($r < 510$ pc for CO and $r < 640$ pc for HCN), but it reaches 0.34 in the smaller aperture (within the central $r < 350 \times 150$ pc region). These CO and HCN properties in NGC 1097 are similar to those in the type-2 Seyfert galaxies NGC 1068 and NGC 5194 (M 51).

Key words: galaxies: active — galaxies: individual(NGC 1097) — galaxies: ISM — galaxies: Seyfert — galaxies: starburst

1. Introduction

The dense molecular medium plays various roles in the vicinity of active galactic nuclei (AGNs). The presence of dense and dusty interstellar matter (ISM), which obscures the broad line regions in AGNs, is inevitable at < 1 pc - a few 10 pc scales according to the proposed unified model of Seyfert galaxies (e.g., Antonucci 1993). These circumnuclear dense ISM could be a reservoir of fuel for the active nuclei, and also be a site of massive star formation.

In fact, strong HCN(1–0) emission, which requires dense ($n_{\text{H}_2} > 10^4 \text{ cm}^{-3}$) environments for its collisional excitation, has been detected in the prototypical type-2 Seyfert NGC 1068 (Jackson et al. 1993; Tacconi et al. 1994; Helfer, Blitz 1995) and the low-luminosity type-2 Seyfert NGC 5194 (Kohno et al. 1996). The HCN(1–0) to CO(1–0) integrated intensity ratios in brightness temperature scale, $R_{\text{HCN/CO}}$, are enhanced up to about 0.4 – 0.6 in these Seyfert nuclei, and the kinematics of the HCN line imply that this dense molecular medium can be outer envelopes of the predicted obscuring material. Nevertheless, our knowledge on the nature of circumnuclear dense molecular matter in Seyfert nuclei has still been very limited. This is because there are only a few high resolution (i.e., a few 100 pc resolution or less) and sensitive observations of dense molecular gas in Seyfert galaxies, although several surveys of dense molecular gas with low resolution instruments have been conducted to address the global quantities of dense molecular gas in the AGN hosts (Papadopoulos, Seaquist 1998; Curran et al. 2000).

In this paper, we report detection of the enhanced HCN emission toward the nucleus of the low luminosity type-1 Seyfert galaxy NGC 1097 using the Nobeyama Millimeter Array (NMA) and NRO 45 m telescope. NGC 1097 is a nearby ($D = 14.5 \text{ Mpc}$, Tully 1988) barred spiral galaxy classified as SB(s)b (de Vaucouleurs et al. 1991) showing double-peaked broad H α emission with time variability at the nucleus (Storchi-Bergmann et al. 1997). The detection of a hard X-ray source at the nucleus (Iyomoto et al. 1996) also supports the presence of a genuine active nucleus, though it is rather a low luminosity one ($L_{2-10\text{keV}} = 3.7 \times 10^{40} \text{ erg s}^{-1}$ at $D = 14.5 \text{ Mpc}$). Two pairs of huge (\sim a few 10 kpc scale) optical jets have been reported yet their nature is still unclear (e.g., Wehrle et al. 1997). In the circumnuclear region of NGC 1097, there is a well-known starburst ring with a radius of $\sim 10''$ or 700 pc, which is luminous at various wavelengths including radio (Hummel et al. 1987), mid-infrared (Telesco et al. 1993), optical (Barth et al. 1995; Quillen et al. 1995; Storchi-Bergmann et al. 1996), near-infrared (Kotilainen et al. 2000), and soft X-ray (Pérez-Olea, Colina 1996). The star formation rate (SFR) in the ring is very high; about $5 M_{\odot} \text{ yr}^{-1}$ from the extinction corrected H α luminosity (Hummel et al. 1987). The host of NGC 1097 seems to have nested bars (Shaw et al. 1993). CO emission in the center of NGC 1097 has been mapped with the NRO 45 m telescope (Gerin et al. 1988) and a molecular ring associated with the starburst ring has been detected, although angular resolution is insufficient to fully resolve the structure. Low resolution ($\sim 1'$) single dish observations of the CO and HCN lines in NGC 1097 are also reported (Helfer, Blitz 1993).

2. Observations and Data Reduction

The NMA observations of CO(1–0) and HCN(1–0) were made during the period from 1999 November to 2000 March. The NMA consists of six 10 m antennas equipped with tunerless DSB SIS receivers. Two antenna configurations (C and D) were used. The backend was the Ultra Wide-Band Correlator (UWBC; Okumura et al. 2000). It was configured to cover 512 MHz (1330 km s^{-1}) at 2 MHz resolution for CO, and to cover 1024 MHz (3480 km s^{-1}) at 8

MHz resolution for HCN. The visibility calibrator 0202-172 (~ 1.1 Jy) was observed every ~ 20 minutes, and 3C454.3 was observed to determine the passband. The resultant CO (HCN) cube has a velocity resolution of 15.6 km s^{-1} (27.2 km s^{-1}) and a typical rms noise of 29 mJy beam^{-1} (6 mJy beam^{-1}) for each channel.

The 45 m telescope observations were performed in 1998 January. CO(1–0) and HCN(1–0) were observed simultaneously using two SIS receivers with side-band rejection filters (S100 and S80). The sky emission was removed by position switching at an offset of $3'$ in azimuth from the center. The pointing accuracy was checked every 1 hour using a SiO maser source. The spectra were acquired with the 250 MHz wide (650 km s^{-1} for CO and 850 km s^{-1} for HCN) acousto-optical spectrometers. Because the velocity width of emission is very large ($\sim 500 \text{ km s}^{-1}$) compared with the spectrometer bandwidth, each spectrum was inspected carefully. After subtracting linear baselines, adjacent channels were smoothed to 10 km s^{-1} for CO and 20 km s^{-1} for HCN. The rms noise level was 16 mK for CO and 3.5 mK for HCN on a T_A^* scale.

3. Results

We display the CO and HCN velocity integrated intensity maps taken with the NMA in figure 1, together with an optical image and the intensity-weighted mean velocity map of CO emission. Strong enhancement of the HCN emission toward the nucleus of NGC 1097 is immediately evident; the CO image shows three major peaks, i.e., the central peak and “twin-peaks” where dust lanes are connected to the circumnuclear starburst ring. On the other hand, the most conspicuous emission comes from the nucleus in the HCN map.

The azimuthally averaged radial distributions of the CO and HCN intensities and the HCN/CO ratios are shown in figure 2. Again it is confirmed that a considerable fraction of CO emission comes from the ring, whereas the HCN is dominated by the nuclear peak. The resultant HCN/CO ratio is very high; it reaches 0.34 within the central $r < 5'' \times 2''$ or 350×150 pc region. Note that the synthesized beams of these NMA observations are elongated along the North to South direction due to the low declination of NGC 1097, and the observed $R_{\text{HCN/CO}}$ is highly smeared with the observing beam. We expect that the line ratio toward the nucleus would increase further with higher angular resolutions. Additional NMA observations with the most extended configuration are in progress, and will be presented in forthcoming papers.

The total CO and HCN fluxes within the NMA field of views were about $690 \pm 20 \text{ Jy km s}^{-1}$ and $67 \pm 2.9 \text{ Jy km s}^{-1}$, respectively. The total CO flux corresponds to the molecular gas mass of $1.4 \times 10^9 M_\odot$ (including He and heavier elements) if a Galactic $N_{\text{H}_2}/I_{\text{CO}}$ conversion factor, $X_{\text{CO}} = 1.8 \times 10^{20} \text{ cm}^{-2} (\text{K km s}^{-1})^{-1}$ (Dame et al. 2001), is applied just for comparison purposes.

We show the CO and HCN spectra toward the center of NGC 1097 taken with the 45 m telescope in figure 3. Integrated intensities of CO and HCN were 96 ± 2.8 and $11 \pm 0.71 \text{ K km s}^{-1}$ on a $T_{\text{MB}} = T_A^*/\eta_{\text{MB}}$ scale. The obtained CO spectrum roughly agrees with the previous

observations (Gerin et al. 1988), but the quality of our data is greatly improved. The HCN-to-CO integrated intensity ratio was 0.11 at the 45 m telescope observing beams ($r < 510$ pc for CO and $r < 640$ pc for HCN).

We compared the NMA fluxes of CO and HCN with 45 m telescope fluxes by convolving the NMA cubes to the same beam sizes as the 45 m observations. We find that the NMA CO flux corresponds to about 0.88 of the 45 m CO flux, and that the NMA HCN flux is mostly the same as the 45 m HCN flux within the errors. Thus, most of the single dish fluxes are recovered by our interferometric observations.

4. Discussion

4.1. Nature of Dense Molecular Gas toward the Seyfert Nucleus

We have detected enhanced HCN emission toward the nucleus of the type-1 Seyfert galaxy NGC 1097. The $R_{\text{HCN/CO}}$ is about 0.11 in the aperture of the 45 m telescope beams ($r < 7.5''$ or 510 pc for CO and $r < 9.5''$ or 640 pc for HCN), but it reaches 0.34 in the smaller aperture (within the central $r < 5'' \times 2''$ or 350×150 pc region), indicating that the nuclear HCN emission is compact compared with the CO emission associated with the nucleus. This is similar to the case of the type-1.5 Seyfert galaxy NGC 3227, where unresolved HCN emission has been detected toward the nucleus although the CO emission is extended across the nuclear region (Schinnerer et al. 2000).

The observed CO and HCN distributions in NGC 1097 show a striking similarity to those in the type-2 Seyfert galaxies NGC 1068 and NGC 5194, where extreme enhancements of $R_{\text{HCN/CO}}$ have been reported (Jackson et al. 1993; Tacconi et al. 1994; Helfer, Blitz 1995; Kohno et al. 1996), though many other Seyferts show no such significant enhancement of $R_{\text{HCN/CO}}$ values even with the high resolution (\leq a few 100 pc) observations (Kohno et al. 1999a, 1999b; Wild, Eckart 2000; Hüttemeister et al. 2000).

What is the nature of this enhanced HCN emission toward some Seyfert nuclei? It is tempting to speculate that a massive starburst occurs in the very nucleus of “the HCN enhanced Seyferts” (i.e., NGC 1068, NGC 5194, and NGC 1097), if we consider the quantitative and spatial correlations between dense molecular gas and massive star-forming regions in star-forming/starburst galaxies (e.g., Solomon et al. 1992; Kohno et al. 1999a). In fact, massive starbursts within the obscuring molecular torus have been proposed (Cid Fernandes, Terlevich 1995), and such intimate cohabitation of powerful nuclear starburst and Seyfert activity has often been claimed in the nuclei of some type-2 Seyferts (e.g., Heckman et al. 1997; González Delgado 1998; Maiolino et al. 1998). Nevertheless, it seems to be too early to jump to that conclusion because the reported high $R_{\text{HCN/CO}}$ in NGC 1068, NGC 5194, and NGC 1097 (0.34 – 0.6) are too high compared with the centers of nearby nuclear starburst galaxies. High resolution observations of local starbursts often show the $R_{\text{HCN/CO}}$ values within the range of

about 0.1 to 0.2 (Downes et al. 1992; Paglione et al. 1995; Helfer, Blitz 1997). These ratios in starburst nuclei are indeed high compared with normal/quiescent galaxies (e.g., Kohno et al. 2002), yet $R_{\text{HCN/CO}}$ values exceeding 0.3 are quite rare (e.g., Sorai et al. 2002).

In the very centers of AGNs, the HCN abundance can be enhanced due to strong X-ray emission from the active nuclei (Lepp, Dalgarno 1996), and this could be related to the observed enhancement of HCN emission in some Seyfert galaxies (Tacconi et al. 1994). Our preliminary results of the HCN/HCO⁺ survey in Seyfert and starburst galaxies imply that the enhanced HCN emissions in the nuclei of NGC 1068, NGC 1097, and NGC 5194 could originate from the X-ray irradiated molecular torii, and they are *not* associated with the nuclear starbursts because the HCN/HCO⁺ ratios in NGC 1068, NGC 5194, and NGC 1097 are abnormally high compared with nuclear starburst galaxies (Kohno et al. 2001).

4.2. Dense Molecular Gas in the Circumnuclear Starburst Ring of NGC 1097

We detected the CO and HCN emissions associated with the circumnuclear starburst ring in NGC 1097. The azimuthally averaged $R_{\text{HCN/CO}}$ is about 0.16 at the radius of the ring. This ratio is comparable to those in the circumnuclear starburst rings of the type-2 Seyfert galaxies NGC 1068 (Helfer, Blitz 1995) and NGC 6951 (Kohno et al. 1999a). Most of the CO and HCN emission is located in the points where offset dust lanes meet the starburst ring. This situation is widely observed in the circumnuclear region of barred spiral galaxies, and is often referred as a “twin-peaks” morphology (Kenney et al. 1992).

Interestingly, there is a spatial shift between CO and HCN twin-peaks; HCN peaks are shifted downstream compared with the CO peaks if we assume trailing spiral arms (i.e., the gas rotates clockwise). This spatial shift between CO and HCN in the circumnuclear ring of barred spiral galaxies are reported in NGC 1530 (non-Seyfert: Reynaud, Downes 1997) and NGC 6951 (type-2 Seyfert: Kohno et al. 1999a). Our CO data suggest the rotation velocity on the plane of the disk is about 330 km s⁻¹ at a radius of 10'' or 700 pc, giving the dynamical time scale $T_{\text{dyn}} \sim 1.3 \times 10^7$ yr. Thus the observed spatial offset between the CO and HCN peaks, about 20° in the azimuth angle, corresponds to a time delay of $\sim (20/360)T_{\text{dyn}} = 7.3 \times 10^5$ yr. This time delay could be related to the time scale of dense molecular gas formation due to gravitational instabilities of the molecular gas (Kohno et al. 1999a).

These results may imply that the same mechanism can govern the star formation in the central \sim kpc regions of both the type-1 and type-2 Seyfert galaxies. It is often claimed that the host galaxies of the type-2 Seyfert nuclei harbor more intense star formation/starburst compared with the type-1 Seyfert hosts (e.g., Maiolino, Rieke 1995; Maiolino et al. 1997). Because the amount of the molecular gas in the type-2 Seyfert hosts seems to be similar to those in the type-1 hosts (Maiolino et al. 1997; Vila-Vilaró et al. 1998), some mechanisms may exists to enhance the star formation efficiency in the type-2 hosts if the putative enhancement of star formation in the type-2 Seyfert galaxies exists. However, our high resolution CO and HCN

images of the type-1 Seyfert galaxy NGC 1097 show striking similarities in the molecular gas distributions and physical properties of the molecular gas in the central kpc regions of both the type-1 and type-2 Seyfert galaxies, though the sample is very limited at this moment. Further surveys of the high resolution molecular lines in type-1 and type-2 Seyferts could provide us with crucial keys whether significant differences on molecular gas properties do exists or not between the Seyfert types.

The authors thank to the anonymous referee for the comments, which improve this paper. We acknowledge the support of the NRO staff for the operation of the telescopes and the continuous efforts in improving the performance of the instruments. Nobeyama Radio Observatory (NRO) is a branch of the National Astronomical Observatory, an inter-university research institute operated by the Ministry of Education, Culture, Sports, Science and Technology, Japan.

References

Antonucci, R. 1993, *ARA&A*, 31, 473

Barth, A. J., Ho, L. C., Filippenko, A. V., & Sargent, W. L. W. 1995, *AJ*, 110, 1009

Cid Fernandes, R., & Terlevich, R. 1995, *MNRAS*, 272, 423

Curran, S. J., Aalto, S., & Booth, R. S. 2000, *A&AS*, 141, 193

Dame, T. M., Hartmann, D., & Thaddeus, P. 2001, *ApJ*, 547, 792

Downes, D., Radford, S. J. E., Guilloteau, S., Guelin, M., Greve, A., & Morris, D. 1992, *A&A*, 262, 424

Gerin, M., Nakai, N., & Combes, F. 1988, *A&A*, 203, 44

Helpert, T., & Blitz, L. 1993, *ApJ*, 419, 86

Helpert, T., & Blitz, L. 1995, *ApJ*, 450, 90

Helpert, T., & Blitz, L. 1997, *ApJ*, 478, 162

Hummel, E., van der Hulst, J. M., Keel, W. C. 1987, *A&A*, 172, 32

Hüttemeister, S., Aalto, S., Das, M., & Wall, W. F. 2000, *A&A*, 363, 93

Jackson, J. M., Paglione, T. D., Ishizuki, S., & Rieu, N. Q. 1993, *ApJ*, 418, L13

Kenney, J. D. P., Wilson, C. D., Scoville, N. Z., Devereux, N. A., & Young, J. S. 1992, *ApJ*, 395, L79

Kohno, K., Kawabe, R., Tosaki, T., & Okumura, S. K. 1996, *ApJ*, 461, L29

Kohno, K., Kawabe, R., & Vila-Vilaró, B. 1999a, *ApJ*, 511, 157

Kohno, K., Kawabe, R., & Vila-Vilaró, B. 1999b, in *The Physics and Chemistry of the Interstellar Medium*, ed. V. Ossenkopf, J. Stutzki, & G. Winnewisser (GCA-Verlag, Herdecke), 34 (astro-ph/9902251)

Kohno, K., Matsushita, S., Vila-Vilaró, B., Okumura, S. K., Shibatsuka, T., Okiura, M., Ishizuki, S., & Kawabe, R. 2001, in *The Central Kiloparsec of Starbursts and AGN: The La Palma Connection*, ed. J. H. Knapen, J. E. Beckman, I. Shlosman, & T. J. Mahoney (ASP, San Francisco), 672 (astro-ph/0206398)

Kohno, K., Tosaki, T., Matsushita, S., Vila-Vilaró, B., & Kawabe, R. 2002, *PASJ*, 54, 541

Kotilainen, J. K., Reunanen, J., Laine, S., & Ryder, S. D. 2000, *A&A*, 353, 834

Lepp, S., & Dalgarno, A. 1996, *A&A*, 306, L21

Maiolino, R., & Rieke, G. H. 1995, *ApJ*, 454, 95

Maiolino, R., Ruiz, M., Rieke, G. H., & Papadopoulos, P. 1997, *ApJ*, 485, 552

Iyomoto, N., Makishima, K., Fukazawa, Y., Tashiro, M., Ishisaki, Y., Nakai, N., & Taniguchi, Y. 1996, *PASJ*, 48, 231

Okumura, S. K., Momose, M., Kawaguchi, N., Kanzawa, T., Tsutsumi, T., Tanaka, A., Ichikawa, T., Suzuki, T., et al. 2000, *PASJ*, 52, 393

Ondrechen, M. P., van der Hulst, J. M., & Hummel, E. 1989, *ApJ*, 342, 39

Paglione, T. A. D., Tosaki, T., & Jackson, J.M. 1995, *ApJ*, 454 L117

Papadopoulos, P. P., & Seaquist, E. R. 1998, *ApJ*, 492, 521

Pérez-Olea D.E., & Colina, L. 1996, *ApJ*, 468, 191

Quillen, A. C., Frogel, J. A., Kuchinsky, L. E., & Terndrup, D. M. 1995, *AJ*, 110, 156

Reynaud, D., & Downes, D. 1997, *A&A*, 319, 737

Schinnerer, E., Eckart, A., & Tacconi, L. J. 2000, *ApJ*, 533, 826

Shaw, M. A., Combes, F., Axon, D. J., & Wright, G. S. 1993, *A&A*, 273, 31

Solomon, P. M., Downes, D., & Radford, S. J. E. 1992, *ApJ*, 387, L55

Sorai, K., Nakai, N., Kuno, N., & Nishiyama, K. 2002, *PASJ*, 54, 179

Storchi-Bergmann, T., Eracleous, M., Ruiz, M. T., Livio, M., Wilson, A. S., & Filippenko, A. V. 1997, *ApJ*, 489, 87

Tacconi, L. J., Genzel, R., Blietz, M., Cameron, M., Harris, A. I., & Madden, S. 1994, *ApJ*, 426, L77

Telesco, C. M., Dressel, L. L., & Wolstencroft, R. D. 1993, *ApJ*, 414, 120

Tully, R. 1988, *Nearby Galaxies Catalog* (Cambridge University Press, Cambridge)

Vila-Vilaró, B., Taniguchi, Y., & Nakai, N. 1998, *AJ*, 116, 1553

Wild, W., & Eckart, A. 2000, *A&A*, 359, 483

Wehrle, A. E., Keel, W. C., & Jones, D. L. 1997, *AJ*, 114, 115

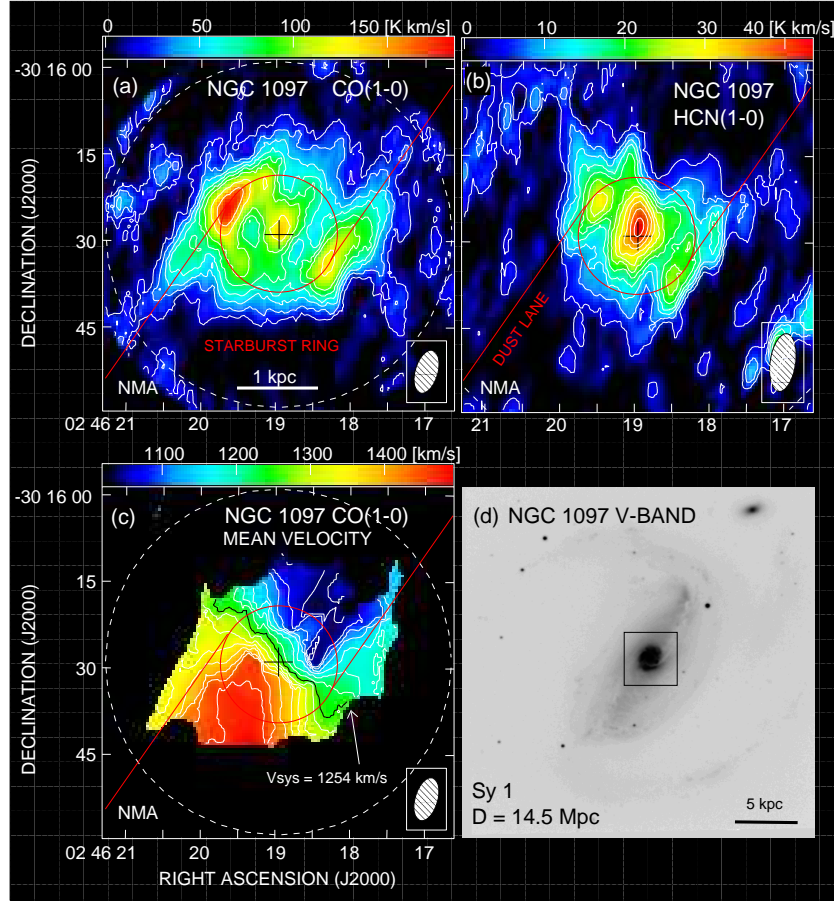


Fig. 1. The NMA maps of CO(1–0) and HCN(1–0) lines, along with the optical image of NGC 1097. The central cross in figure 1a, 1b, and 1c marks the peak of 6 cm continuum (Hummel et al. 1987). The coordinate is $\alpha(\text{J2000}) = 02^{\text{h}}46^{\text{m}}18^{\text{s}}96$ and $\delta(\text{J2000}) = -30^{\circ}16'28.9"$. In each molecular map, the NMA field of view (60" for CO and 80" for HCN) is indicated by a dashed circle. The circumnuclear starburst ring with a radius of $r \sim 10''$ or 700 pc is shown by a red circle, and two red lines indicate the dust lanes along the bar. Attenuation due to primary beam pattern of each 10 m dish has been corrected in these maps. (a) Integrated intensity map of CO. The synthesized beam is $7.''7 \times 3.''9$ (540 \times 270 pc) with a P.A. of -16° . The contour levels are 1.5, 3, 4.5, 6, 7.5, 9, 12, 15, and 18 σ , where $1 \sigma = 3.39 \text{ Jy beam}^{-1} \text{ km s}^{-1}$ or 10.4 K km s^{-1} in T_b . This corresponds to a face-on gas surface density Σ_{gas} of $20.8 M_{\odot} \text{ pc}^{-2}$, calculated as $\Sigma_{\text{gas}} = 1.36 \times \Sigma_{\text{H}_2}$ and $\Sigma_{\text{H}_2} = 2.89 \cos i \times (I_{\text{CO}} / \text{K km s}^{-1})$, where I_{CO} is the velocity-integrated CO intensity and i is the inclination of the disk (46° for NGC 1097; Ondrechen et al. 1989). (b) Integrated intensity map of HCN. The synthesized beam is $10.''1 \times 4.''4$ (710 \times 310 pc) with a P.A. of -8° . The contour levels are 1.5, 3, 4.5, \dots , 15, and 16.5 σ , where $1 \sigma = 0.711 \text{ Jy beam}^{-1} \text{ km s}^{-1}$ or 3.54 K km s^{-1} in T_b . (c) Intensity-weighted mean velocity map of CO. The contour interval is 30 km s^{-1} , and the systemic velocity of 1524 km s^{-1} , determined by the fitting of this CO data, is indicated. Circular rotation seems to dominate the kinematics in the central $r < 10''$ region (i.e., within the circumnuclear ring) in NGC 1097, whereas very strong non-circular motions along the dust lanes are suggested by isovelocity contours nearly parallel to the dust lanes. (d) A V-band image of NGC 1097 (Quillen et al. 1995). The central $400'' \times 400''$ (28 kpc \times 28 kpc) region is displayed. A solid box indicates the area of the CO and HCN maps (60'' \times 60'').

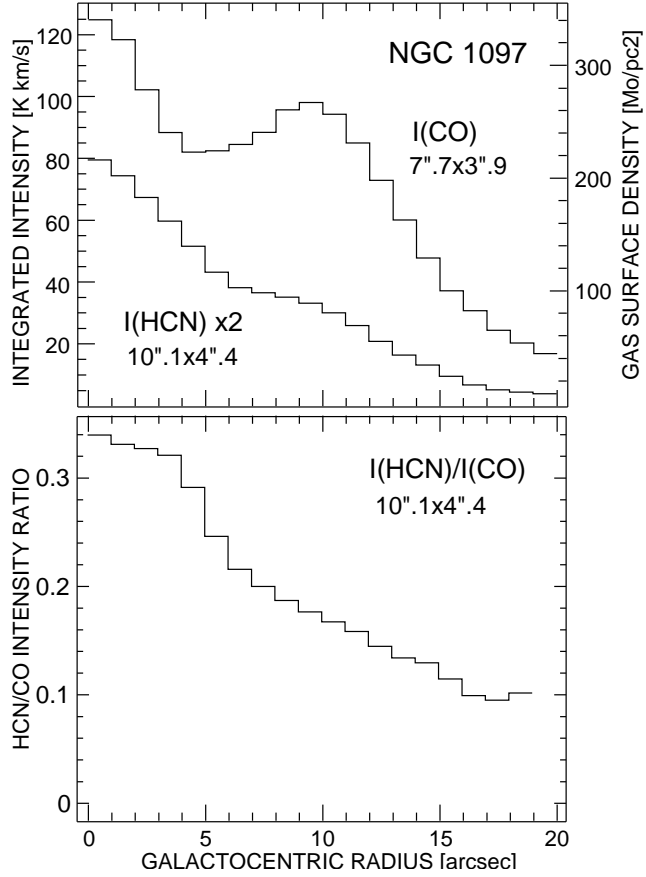


Fig. 2. Azimuthally averaged radial distributions of CO and HCN (top right), and the HCN/CO ratios (bottom right) in NGC 1097. The systematic errors of the radial distributions and the ratio are about $\pm 10\%$. The face-on gas surface densities from the CO intensities are also indicated, assuming X_{CO} of $1.8 \times 10^{20} \text{ cm}^{-2} (\text{K km s}^{-1})^{-1}$.

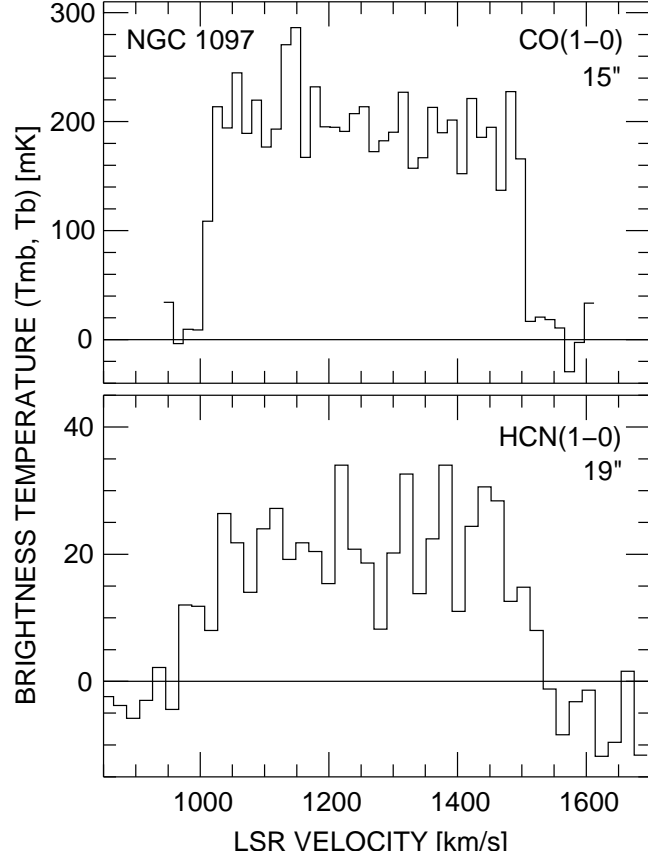


Fig. 3. CO and HCN spectra in the center of NGC 1097 obtained with the NRO 45 m telescope, displayed in the main-beam temperature scale ($T_{\text{MB}} \equiv T_{\text{A}}^*/\eta_{\text{MB}}$). The beam sizes (HPBW) of CO and HCN observations are $15''$ and $19''$, respectively. The main-beam efficiencies (η_{MB}) were 0.45 ± 0.03 for CO and 0.50 ± 0.03 for HCN observations.